Lesion-Symptom Mapping of the Human Cerebellum

72

Dagmar Timmann, Michael Küper, Elke R. Gizewski, Beate Schoch, and Opher Donchin

Abstract

Although the function of the cerebellum cannot be inferred from lesion data alone, it is still of major scientific and clinical interest to assess whether lesions of a given cerebellar area lead to specific behavioral deficits. The introduction of high-resolution structural brain imaging and new analysis methods has lead to significant improvement in the ability to draw such conclusions. Lesion-symptom mapping is now possible with a spatial resolution at the level of individual lobules and nuclei of the cerebellum. The investigation of patients with defined focal lesions yields the greatest potential for obtaining meaningful correlations between lesion site and behavioral deficits. In smaller groups of patients, overlay plots and subtraction analysis are good options. If larger groups of patients are available, different statistical techniques have been introduced to

D. Timmann (✉) • M. Küper
Department of Neurology, University of Duisburg-Essen, Hufelandstrasse 55, Essen, 45147, Germany
e-mail: dagmar.timmann-braun@uni-duisburg-essen.de, michael.kueper@uni-duisburg-essen.de

E.R. Gizewski
Departments of Neuroradiology, University of Duisburg-Essen and Justus-Liebig-Universität Gießen, Klinikstr. 33, Gießen, 35385, Germany
e-mail: elke.gizewski@radiol.med.uni-giessen.de

B. Schoch
Departments of Neurosurgery, University of Duisburg-Essen and Stiftungsklinikum Mittelrhein GmbH, Johannes-Müller-Straße 7, Koblenz, 56068, Germany
e-mail: beate.schoch@stiftungsklinikum.de

O. Donchin
Department of Biomedical Engineering and Zlotowski Center for Neuroscience, Ben-Gurion University of the Negev, Be'er Sheva, 84105, Israel
e-mail: donchin@bgu.ac.il

M. Manto, D.L. Gruol, J.D. Schmahmann, N. Koibuchi, F. Rossi (eds.),
Handbook of the Cerebellum and Cerebellar Disorders,
DOI 10.1007/978-94-007-1333-8_72,

compare behavior and lesion site on a voxel-by-voxel basis. Although localization in degenerative cerebellar disorders is less accurate because of the diffuse nature of the disease, certain information about the supposed function of larger subdivisions of the cerebellum can be gained. This review highlights the current developments of lesion-symptom mapping in human cerebellar lesion studies. Examples are given which show that meaningful correlations between lesion site and behavioral data can be obtained both in patients with degenerative as well as focal cerebellar disorders.

Introduction

A traditional approach to elucidate the functions of the human brain, and the cerebellum in particular, is to study impairment in human subjects with brain lesions. For many years, however, localization of function played only a secondary role in human cerebellar lesion studies. Behavioral abnormalities helped to understand the functions of the cerebellum, but few attempts were made to localize functions within the cerebellum. Localization of functions was hampered by three main reasons. Firstly, many studies are based on small numbers of patients with different etiologies because patients with lesions circumscribed to the cerebellum are rare. Study populations frequently include both focal lesions and degenerative disorders preventing a meaningful comparison of lesion localization and related dysfunction. Secondly, often no or only low-resolution brain imaging data were available. Thirdly and may be most importantly, easy accessible methods to perform lesion-symptom mapping on a group level had not been developed.

Although recruitment of large and homogeneous cerebellar patient populations remains a major challenge, methods to localize function in the cerebellum have much improved in recent years. Magnetic resonance (MR) scanners have become widely available. High-resolution structural MR images (MRI) can be acquired at the same time as behavioral studies are performed or are already performed as part of the diagnostic clinical work-up. Equally important, newer analysis methods have been developed to perform lesion-symptom comparisons (Rorden and Karnath 2004; Rorden et al. 2007, 2009). Initially introduced for patients with cerebral stroke, specific adjustments developed very recently for cerebellar lesion studies have become available (Diedrichsen 2006; Diedrichsen et al. 2009, 2011). Lesion-symptom mapping, which is also called lesion-behavior mapping (Rorden et al. 2009), is now possible with a spatial resolution at the level of individual lobules and nuclei of the cerebellum. As yet, comparatively few studies have used these advanced imaging techniques to study lesions of the human cerebellum and their associated symptoms (Timmann et al. 2009 for review; Baier et al. 2010). This chapter will summarize the methodology of MRI-based lesion-symptom mapping of the human cerebellum and discuss its potential for gaining insights into cerebellar functions. In its first part, the pros and cons of available human cerebellar lesion conditions will be discussed. In the second part, examples of MRI-based lesion-symptom mapping both in focal cerebellar disorders and cerebellar degeneration will be given.

Human Cerebellar Lesion Conditions

In principal, lesions need to be exclusively restricted to the cerebellum in order to infer possible cerebellar functions based on lesion localization and volume. However, patients with lesions restricted to the cerebellum are rare, and it can be argued that there are no patients with 100% pure cerebellar lesions. Yet, several conditions lead to lesions that primarily affect the human cerebellum. In general, three patient groups can be distinguished: patients with focal lesions due to stroke, patients with focal lesions due to (benign) tumors, and patients with slowly progressive degenerative disorders (Timmann et al. 2009). Each of the available human cerebellar lesion conditions has its specific limitations, which will be discussed below.

Cerebellar Stroke

Patients with cerebellar stroke provide the only human lesion condition where symptoms can be studied following an acute lesion in a previously healthy cerebellum. Although tumor surgery causes an acute cerebellar lesion, the growing tumor has caused cerebellar dysfunction for an unknown time. Infarction of the cerebellum is a rare event representing up to 15% of all cerebral strokes (Tohgi et al. 1993; Amarenco 1991). First with the introduction and later with better availability and quality of CT and MRI scanners, the number of detected cerebellar infarcts has increased. Furthermore, it became clear that the "classical" cerebellar ischemic syndromes including brainstem signs as well as life-threatening brainstem compression and hydrocephalus from postinfarct edema are comparatively rare (Kase et al. 1993; Chaves et al. 1994). The majority of cerebellar infarctions have a benign clinical course.

The main cerebellar arteries are the posterior inferior cerebellar artery (PICA), the anterior inferior cerebellar artery (AICA), and the superior cerebellar artery (SCA) (Fig. 72.1; Caplan 1996). Branches of the PICA supply the inferior aspects of the cerebellar hemispheres and inferior vermis extending up to the primary horizontal fissure. Branches of the AICA supply the flocculus and adjacent lobules of the inferior and anterior cerebellum and the middle cerebellar peduncles. The SCA supplies the superior parts of the cerebellum down to the horizontal fissure. It supplies all cerebellar nuclei and most of the cerebellar white matter. In some cases, the PICA supplies parts of the dentate nucleus. The cerebellar vascular territories are nicely illustrated in Tatu et al. (1996) based on pathological studies by Amarenco (1991) and the injection studies by Marinkovic et al. (1995).

Symptoms and signs differ depending on the vascular territory. Infarction in the territory of any of the three cerebellar arteries results in limb and gait ataxia (Kase et al. 1993; Tohgi et al. 1993). Dysarthria is a characteristic finding in SCA distribution infarcts, whereas vertigo is particularly common in infarcts in the PICA and AICA territories (Kase et al. 1993; Urban et al. 2001). SCA and PICA infarcts are most common and occur with similar frequency (about 40% each; Caplan 1996). AICA infarcts are rare (about 10%). Whereas PICA and SCA infarcts are frequently restricted to the cerebellum, AICA territory infarcts almost always

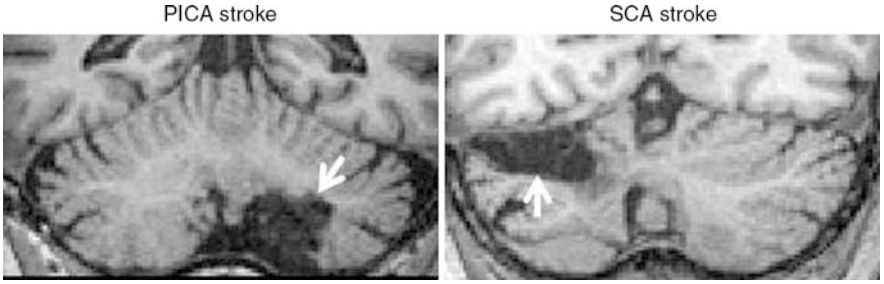

Fig. 72.1 Coronal views of T1-weighted MR images of a chronic posterior inferior cerebellar artery (PICA) infarct (*left*) and a chronic superior cerebellar artery (SCA) infarct (*right*)

include the lateropontine area and brainstem signs predominate (Amarenco et al. 1993; Barth et al. 1993).

In sum, patients with lesions in the PICA and SCA territories are a suitable condition to study lesion-symptom mapping in the cerebellum. Lesion effects on brainstem and the possibility of accompanying cerebral vascular disease need to be excluded, but often the lesions are relatively pure. SCA and PICA patients tend to be more restricted to the cerebellum, while AICA infarcts are rare and commonly affect the brainstem.

Cerebellar Tumors

While patient availability may require the pooling of subjects with cerebellar ischemic lesions and cerebellar tumors, one needs to recognize several caveats that may limit the usefulness of pooling (Anderson et al. 1990). The first caveat concerns the age of the patient population. Whereas ischemic stroke is typically a disease of late adulthood, benign cerebellar tumors occur most frequently in children (ca. 75%; Rashidi et al. 2003). Furthermore, unlike the adult situation where brain tumors are most often malignant primary or secondary neoplasms, in children, at least half of the brain tumors are benign. In children, the most frequent cerebellar tumors are pilocytic astrocytomas (WHO grade 1; ca. 35–40%) and medulloblastomas (ca. 40%). For the study of cerebellar function, the investigation of patients with benign astrocytomas is much preferred. Complete surgical removal of the tumors cures the disease in the majority of cases. For malignant medulloblastoma, however, additional chemotherapy and radiation are needed with known detrimental effects on brain function particularly in young children.

Findings in these patients may be confounded by ongoing central nervous system maturation. Although most postnatal development of the cerebellum takes place within the first year or two of life and the cerebellum reaches adult size at 4–7 years of age (Giedd et al. 1996; Brain Development Cooperative Group 2011), myelinization continues at a slow rate in subsequent years most likely until young adulthood (Pfefferbaum et al. 1994). However, the sequence of myelinization is

thought to follow the order of phylogenetic development (Vogt 1905). Older parts of the cerebellum (i.e., archi- and paleocerebellum) probably complete myelinization earlier than newer parts (i.e., neocerebellum) (Jernigan and Tallal 1990).

One pathology in young adults that does admit study are benign, noninvasive vascular tumors, in particular hemangioblastomas (WHO grade I), both sporadic or as part of Hippel-Lindau disease, and arteriovenous malformations (AVMs) of the cerebellum (Conway et al. 2001). The majority of hemangioblastomas occur within the cerebellar hemispheres, whereas AVM malformations more frequently affect the cerebellar vermis. However, these conditions are rare, and a large group of subjects is usually difficult to amass without the close cooperation of a specialized center.

Apart from age, a second difference between tumor pathologies and ischemic stroke is that benign cerebellar tumors grow slowly, whereas stroke has an acute onset. In pilocytic astrocytomas, symptoms often progress insidiously during a period of months, or in some cases years, before diagnosis. This allows compensation to take place. In fact, clinical presentation typically involves signs of increased intracranial pressure including headache, vomiting, and papilledema. Cerebellar signs are less frequently present at the time of diagnosis. Often, ataxia only manifests after removal of the tumor, possibly due to the acute surgical lesion.

In order to perform lesion-symptom mapping in tumor patients, it is best to test behavior in the chronic stage after surgical removal of the tumor. Because many cerebellar tumors cause symptoms due to mass effects (e.g., due to accompanying cysts in pilocytic astrocytoma and hemangioblastoma), exact lesion site is difficult to determine with the tumor still in place (Karnath and Steinbach 2011). In acute surgical lesions, there is usually a significant shift in neuronal structures because of edema, air, and cell detritus (see also section "Acute Cerebellar Lesions" below). Furthermore, mass effects may cause accompanying hydrocephalus. The long-term effects of hydrocephalus and sudden surgical decompression are difficult to control.

A third difference between tumors and ischemia strokes is lesion localization. Cerebellar astrocytomas involve the vermis and cerebellar hemispheres with approximately equal frequency (Zuzak et al. 2008). In contrast with ischemic strokes, which affect both superior and inferior parts of the cerebellum, tumors are most frequently located within the posterior lobe.

In summary, young adults who have had operations on pilocytic astrocytomas in childhood or youth are a good option to study lesion-symptom mapping in the cerebellum. Younger and otherwise healthy subjects are an advantage compared to the majority of ischemic stroke patients. However, effects of increased intracranial pressure and a slowly growing lesion with subsequent removal in a still maturating brain complicate interpretation and are difficult to control. Young adults with removal of benign vascular tumors provide another possible condition, but patients are rare.

Cerebellar (Cortical) Degeneration

Only a subset of hereditary, nonhereditary, and acquired degenerative ataxias are considered "pure" cerebellar disorders (Durr 2010). Spinocerebellar ataxia type 6

(SCA6; a hereditary form of ataxia) and sporadic adult onset ataxia (SAOA; a nonhereditary form) are the best known examples. The neuropathological hallmark is cerebellar cortical degeneration, mostly affecting the Purkinje cell layer (Sasaki et al. 1998; Yang et al. 2000). Although some degenerative disorders affect the cerebellar nuclei (e.g., dentate nucleus in Friedreich's ataxia and spinocerebellar ataxia type 3, SCA3), these disorders affect various other parts of the nervous system. The degenerative cerebellar disorders are slowly progressive disorders. Ongoing cerebellar degeneration and development of compensatory mechanisms and reorganization in both cerebellar and cerebral areas are likely to progress simultaneously.

As a rule of thumb, autosomal recessive ataxias (e.g., Friedreich's ataxia) present with significant extracerebellar involvement – mostly spinal cord degeneration and significant polyneuropathy – and should not be used in studies of cerebellar function. Prior to the introduction of genetic tests, the autosomal dominant ataxias had been classified by Anita Harding into three groups based on the phenotype: ADCA type I, II, and III. The most common phenotype is ACDA type I which is accompanied by varying extracerebellar symptoms. ADCA type II is rare and accompanied by visual loss. The second most common form is ADCA type III which is a purely cerebellar syndrome. Although the Harding classification has been replaced by the genetic classification of spinocerebellar ataxias (SCA), it is still useful particularly in cases where genetic testing has been inconclusive. ADCA III, but not ADCA I and II, may be included in lesion studies. The most common SCAs are SCA1, SCA2, SCA3, and SCA6, which account for up to 75% of all SCA families (Klockgether 2008). Whereas SCA1, SCA2, and SCA3 are ADCA type I, SCA6 is the prototype of ADCA type III. Thus, patients with SCA1, SCA2, and SCA3 should be excluded from lesion studies while SCA6 patients can be useful subjects for these studies. For some other, rare forms, a benign course with a more cerebellar phenotype has been described as well (Schöls et al. 2008; Durr 2010).

SCA6 is a disorder of late adulthood, with a mean age of onset of 50–60 years (30–70, mean 50), and it is not always purely cerebellar. A subset of patients develops mild signs of axonal polyneuropathy (pallhypesthesia) and pyramidal tract dysfunction (brisk tendon reflexes). Sleep disorders and mild dysphagia may also occur (Rüb et al. 2006). The same is true for sporadic adult onset ataxia (SAOA), which has a similar clinical and MRI presentation as SCA6 (Abele et al. 2007). In this case, family history and genetic testing are negative, and the underlying cause is unknown. SAOA has previously been named idiopathic cerebellar ataxia (IDCA) and idiopathic late-onset cerebellar ataxia (ILOCA). During the course of the disease, patients need to be carefully monitored for autonomic and extrapyramidal signs and the development of pontine atrophy and hyperintensities in the brainstem. Indeed, a percentage of the patients develop multiple system atrophy type C (MSA-C) and need to be excluded from further behavioral studies.

Paraneoplastic cerebellar degeneration and viral cerebellitis may present with pure cerebellar degeneration. In contrast to the hereditary and nonhereditary degenerative ataxias, degeneration is subacute with very little time for compensation and reorganization. Subjects are severely affected within days or weeks. In the acute

stage, lesion-symptom mapping is limited because early brain scans do not reveal cerebellar atrophy. In paraneoplastic disorders, testing can be further limited by the underlying malign disorder.

In sum, the most common "pure" cerebellar ataxias are spinocerebellar ataxia type 6 (SCA6), which is autosomal dominantly inherited, and sporadic adult onset ataxia (SAOA). Although there are exceptions, these disorders commonly occur in the elderly. Other limitations (mild extracerebellar involvement in some patients) apply.

Lesion-Symptom Mapping

Lesion-symptom mapping leads to promising results both in patients with focal cerebellar disorders and in patients with cerebellar degeneration (Timmann et al. 2009 for review). Studies of patients with focal lesions are commonly preferred because lesion-symptom maps are more precise than in studies of patients with degenerative diseases. Focal lesions are better defined than in cerebellar degeneration which affects the whole cerebellum although to various degrees. Furthermore, a chronic (and acute lesions for most part) focal lesion can be delineated as a cerebellar region with complete lack of function. Volumetry and gray matter density measures, which quantify the degree of degeneration, need to be made in degenerative disease. These measures likely reflect cerebellar physiological dysfunction only in part. However, access to patients with degenerative cerebellar disorders is generally easier. Disorders are progressive and patients show significant behavioral disorders. This is different to chronic focal disease, where remaining dysfunction is usually minor due to compensation. Therefore, it is of interest to perform lesion-symptom mapping in patients with degenerative disease.

Focal Cerebellar Disorders

Until recently, few studies took advantage of lesion localizations in their study designs. Some studies compared patients with lesions affecting the right and left cerebellum (Ravizza et al. 2006; Leggio et al. 2008), lesions affecting primarily the midline (vermis) or hemispheres (Riva and Giorgi 2000; Steinlin et al. 2003), or those affecting either PICA or SCA territory (Exner et al. 2004). In the more recent years, an increasing number of studies apply advanced imaging tools of lesion-symptom mapping, which will be outlined below.

Structural MRI Sequences and Delineation of Focal Lesions

Chronic Cerebellar Lesions

Lesion delineation is most straight forward in patients with chronic stroke and in the chronic stage after surgical tumor removal. However, the drawback is that plastic changes have occurred and behavior is confounded by compensatory effects. In addition, secondary changes, such as focal cerebellar cortical atrophies following

surgical lesions, can also occur. Despite the good quality of new generation computerized tomography (CT), magnetic resonance imaging (MRI) is the method of choice for visualization of structures within the posterior fossa. Chronic focal lesions are hypointense on T1-weighted MRI images and generally well demarcated (Fig. 72.1). Lesions are traced directly on axial, sagittal, and coronal slices of 3D high-resolution MRI data. However, if high-resolution MRI is not available, lesions can be manually transferred from lower-resolution MRI or CT images onto 3D high-resolution templates of the cerebellum (see below) using anatomical landmarks (Baier et al. 2009, 2010).

Most commonly magnetization-prepared rapid gradient echo (MPRAGE) images with a spatial resolution of 1 mm isotropic voxel size are acquired on 1.5 T or 3 T MR scanners. Additional MRI sequences can be helpful to exclude extracerebellar lesions or make decisions of lesion extent easier. For example, fluid attenuation inversion recovery (FLAIR) images are very sensitive to show white matter lesions (Barkhof and Scheltens 2002). The gold standard of lesion delineation is manual tracing. This is most commonly done on the nonnormalized T1-weighted MRI scans using image processing software such as the freely available MRIcro (www.cabiatl.com/mricro/) or MRIcron (www.cabiatl.com/mricro/mricron/). Intra- and interobserver reliability has been assessed for ischemic cerebral stroke and showed high agreement within and between observers (Fiez et al. 2000). There have been attempts to automatically or semiautomatically trace chronic cerebral stroke (Seghier et al. 2008; Wilke et al. 2011). One reason being to get more objective, user-independent results and the other to circumvent the time-consuming manual tracing. Although these methods appear to work generally well for larger lesions and lesions which are located more centrally in the brain, they work less well for smaller lesions and lesion located more in the periphery (Wilke et al. 2011). Thus, manual tracing remains the gold standard.

Acute Cerebellar Lesions

Studies are most commonly performed in patients with chronic focal lesions. Studies in patients with acute cerebellar lesions imply a prospective study design (i.e., the study must be designed before the subject pool is determined and then patients collected as they become available). Because patients are rare, data need to be collected over the course of a couple of years unless studies are performed in multiple centers simultaneously. Patients should be included at the same time after the insult to exclude the influence of different compensation stages on behavior (Rorden et al. 2009). Additionally, the site of the lesion is more difficult to define in acute than in chronic patients. This is particularly true in surgical lesions. In acute surgical lesions, there is usually a significant shift in neuronal structures because of edema, air, and cell detritus. This causes overestimation of the extent of the lesions. Then, spatial normalization of the MRI data is difficult because individual landmarks are not stable after surgery. Furthermore, edema causes difficulty in differentiating between the effects of permanent and temporary lesions.

Edema and shift of anatomy are usually not a problem in acute stroke. In acute stroke, however, special MRI sequences are needed to show the full extent of the lesion. In very early stages, lesions may only be visualized on diffusion-weighted

(DWI) or fluid-attenuated inversion recovery (FLAIR) images (Wintermark et al. 2008). Therefore, DWI should be performed in the first 48 h after stroke and FLAIR MRI after 48 h in the acute stage (Karnath et al. 2005; Baier et al. 2009, 2010; Baier and Dieterich 2011). DWI allows good prediction of final infarct size. In the acute stage, however, some areas are structurally intact but not functioning normally. Here, perfusion MRI is helpful. This, however, requires injecting gadolinium during MRI scans or applying arterial spin labeling to use the blood itself as a contrast agent (Rorden and Karnath 2004).

Furthermore, both in acute ischemic and surgical lesions, distant regions not affected by the structural lesions might suffer impaired function because of sudden loss of input. Single photon emission computed tomography (SPECT) or positron emission tomography (PET) allow visualization of disconnected areas, but because they are invasive techniques, they are rarely available. In the future, diffusion tensor imaging (DTI) may provide information about disconnected areas.

Cerebellar Nuclei

T1-weighted MR images work well to show chronic lesions of the cerebellar cortex, but the cerebellar nuclei are not visible. Acquisition of additional MRI sequences allows visualization of the cerebellar nuclei (Küper et al. 2010 for review). The iron content is high in the cerebellar nuclei. The paramagnetic properties of iron result in variations in the volume susceptibility. These iron-induced artifacts can be shown as hypointensities on T2 (spin-echo)- and T2* (gradient-echo)-weighted images (see, for example, Figs. 72.4 and 72.6). Susceptibility-weighted imaging (SWI) is a newer method which can be used to visualize the cerebellar nuclei (Diedrichsen et al. 2011). Another option is quantitative T1 and proton density imaging (Deoni and Catani 2007). Although the dentate nuclei can be visualized using SWI at 1.5 T with reasonable precision, 3 T (or even 7 T) imaging is of advantage to depict the fine structure of the cerebellar nuclei. Firstly, iron-induced susceptibility artifacts increase with increasing field strength. Secondly, increased field strength allows for an increase in spatial resolution. In a recent study, SWI performed on a 7 T scanner was used to differentiate between the dentate, interposed, and fastigial nuclei in individual healthy subjects (Fig. 72.2; Diedrichsen et al. 2011). It will be of interest to use SWI imaging in patients with focal cerebellar lesions to determine which parts of the nuclei are affected in future studies.

Normalization of the Cerebellar Cortex and Nuclei

Lesion-symptom mapping is done on a group level. In order to compare lesion sites and behavior on a group level, it is necessary that cerebellar lesions are transformed in a common stereotactic space (“normalized”). That is, lesions are deformed to fit a standard template of the brain. The same principle applies for functional brain imaging. For many years, the standard MNI brain template provided in SPM was used to normalize the cerebellum (http://www.fil.ion.ucl.ac.uk/spm/). The MNI template, however, has limited information about the finer structure of the cerebellum. In 2006, Diedrichsen has published a spatially unbiased atlas template of the human cerebellum (SUIT). The SUIT template significantly improves the overlap

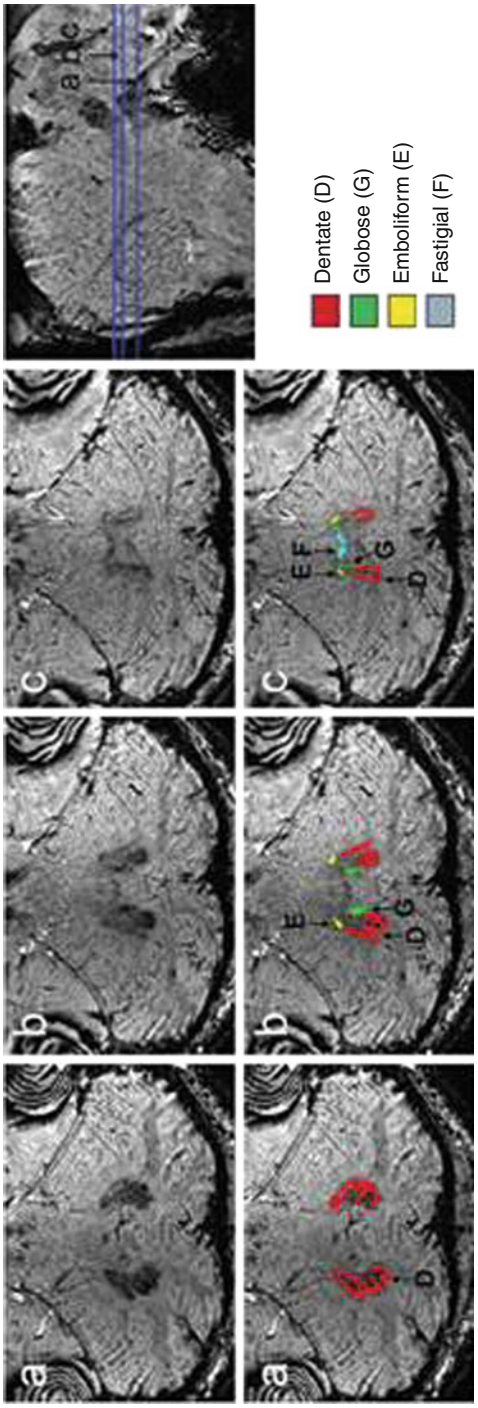

Fig. 72.2 Cerebellar nuclei in a healthy individual shown on susceptibility-weighted images (7 T, 0.5 mm isotropic resolution). Three horizontal slices are shown without (*upper row*) and with (*lower row*) drawings displayed. *Red* – dentate nucleus, *green* – globose nucleus, *yellow* – emboliform nucleus, *blue* – fastigial nucleus (Reprinted from Diedrichsen et al. 2011, Fig. 2, with permission from Elsevier)

of functionally equivalent cerebellar regions across individuals compared to standard templates in SPM. SUIT normalization considers only the cerebellum (and adjacent brainstem) and uses a template with more anatomical information of the cerebellum. The method is called spatially unbiased because "the location of each structure is equal to the expected location of that structure across individuals in MNI space" (www.icn.ucl.ac.uk/motorcontrol/imaging/suit.htm). SUIT has been designed as a toolbox for SPM and is freely available. Initially, the cerebellum and brainstem have to be isolated from the surrounding tissue. Thereafter, the cerebellum and the traced lesion are simultaneously spatially normalized into SUIT atlas space. Normalization of the cerebellum is performed while the lesioned region plus a safety margin is ignored according to the masking technique introduced by Brett et al. (2001).

Although SUIT has improved not only the normalization of the cerebellar cortex (SUIT template shows anatomical detail for the cortex only) but also for the cerebellar nuclei, SUIT has recently been extended for specific normalization of the dentate nuclei (/www.icn.ucl.ac.uk/motorcontrol/imaging/suit_function.htm#suit_normalize_dentate). This normalization algorithm tries to deform the T1 image so that it fits to the SUIT template, while optimizing the overlap between the dentate nucleus and a template of the cerebellar nuclei that has been developed as an average of 23 healthy control subjects (Diedrichsen et al. 2011). To perform the latter, the dentate nucleus is manually traced on T2*-weighted or SWI images and saved as region of interest. This method ensures a near-perfect overlap between the nuclei of individual participants, while preserving a good normalization of other structures. This method has been applied for functional MRI data (Küper et al. 2011a; Thürling et al. 2011) but can equally be used for structural data. Both the dentate nucleus and possible lesions of the dentate can be drawn manually in SWI images. This method will improve lesion-symptom mapping of the dentate nucleus in future studies. As yet, the cerebellar nuclei are usually not directly visualized. Whether the cerebellar nuclei are affected or not is decided with the help of atlases (see section "Atlases of the Cerebellar Cortex and Nuclei" below) in data sets normalized to MNI or SUIT space.

Statistical Analysis in Focal Cerebellar Lesions

In smaller groups of subjects, lesion overlay plots and subtraction analyses are useful approaches. Lesion overlay of patients showing the same disorder is the simplest form of data analysis. If lateralization is not part of the scientific question, lesions are frequently mirrored to the same side of the cerebellum for better comparison. A more advanced method is the comparison of lesion site between two groups of patients with and without impairment in a given task (Rorden and Karnath 2004). Likewise, patients can be divided into a group with and a group without lesion in a specific area, and then, behavior can be compared between the two groups. If larger groups of patients with focal lesions are available, innovative statistical techniques have been introduced to compare behavior and lesion site on a voxel-by-voxel basis (Bates et al. 2003; Rorden and Karnath 2004; Rorden et al. 2007, 2009).

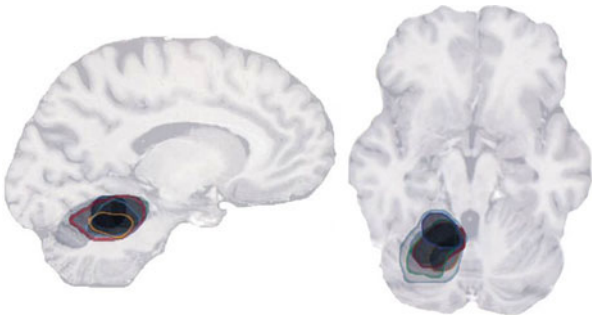

Fig. 72.3 *Superimposition of lesions in patients with the same disorder* (Reprinted from Urban et al. 2001, Fig. 2, with permission from Wolters Kluwer Health). Superimposed cerebellar ischemic lesions in six patients leading to dysarthria. Lesions are superimposed on sagittal and axial MRI scans of a healthy subject. Lesions are flipped to the same side

Superimposition of Lesions in Patients Showing the Same Disorder

The simplest use of normalized lesions is to collect patients with the same disorder and superimpose lesions. In the classic study of cerebellar dysarthria by Lechtenberg and Gilman (1978), lesion outlines based on radiographic, surgical, and autopsy findings were transferred onto a schematic drawing of the cerebellum. In a later study, Urban et al. (2001) used more advanced techniques. Lesions were defined on MRI scans, normalized and projected into MR sections of a healthy subject. In both studies, lesion overlaps showed that paravermal regions of the superior cerebellum were related to dysarthria (Fig. 72.3). Only patients who presented with dysarthria were included. Because locations of brain damage are not randomly distributed, simple overlay plots may be biased, that is, they may simply show commonly damaged areas (Rorden and Karnath 2004). The introduction of a control patient group, which does not show the salient behavior, is helpful to substantiate the findings of simple lesion overlays.

Comparing Lesion Site in Two Groups of Patients

There are different ways to compare superimposition of normalized lesions in two groups (Rorden and Karnath 2004). One possibility is to pool brain imaging data across predefined anatomical regions. Another way is to group patients based on a cutoff value of a measured behavioral variable and use this criterion to group the lesion data. The simplest is to create maps of lesion overlap across these predefined groups. Subtraction analysis can help to visualize anatomical trends in these situations (Karnath et al. 2002). These analyses are useful for smaller groups of subjects. This is frequently the case in cerebellar lesion studies because patients with circumscribed focal cerebellar lesions are rare.

Pooling Brain Images Across Predefined Anatomical Regions. The superior and posterior inferior cerebellum is supplied by two different arteries (SCA and PICA, see above). Although there is variability in the territory of the two arteries between subjects, comparison of behavior following PICA and SCA stroke can be useful.

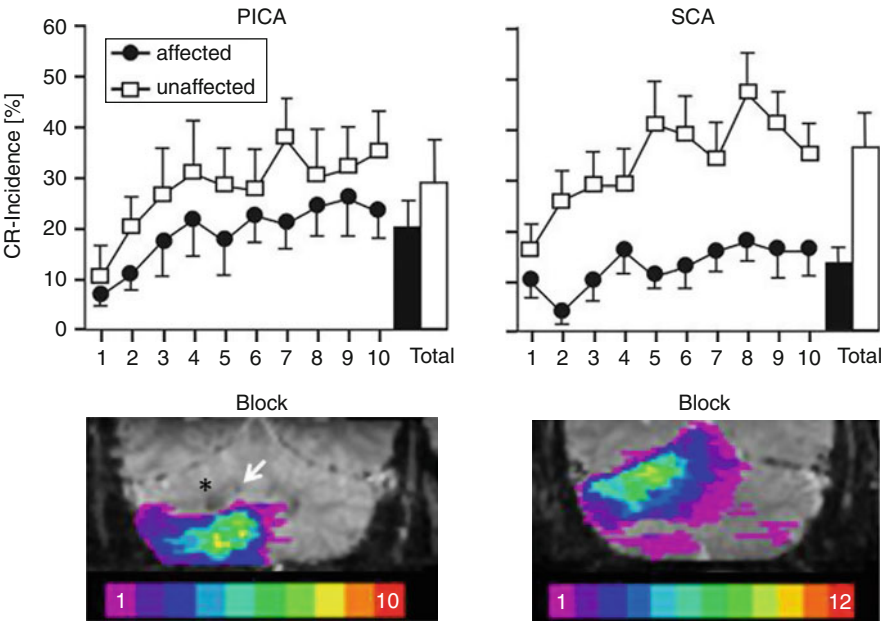

Fig. 72.4 *Pooling brain images across predefined anatomical regions. Upper row*: Eyeblink conditioning in groups of patients with unilateral lesions (i) within the territory of the PICA (*left*) and (ii) within the territory of the SCA (*right*) (Gerwig et al. 2003). Acquisition of conditioned eyeblink responses (CRs) was compared between the affected (*filled circles* and *columns*) and unaffected (*open circles* and *columns*) sides. Mean percentage CR incidences ± SE are shown for each of ten blocks of paired (CS = tone, US = air puff) trials with ten trials per block and across all trials ($n = 100$, total). Note marked reduction of CRs on the affected side in the SCA patients. *Lower row*: Lesions of the PICA patients (*left*) and SCA patients (*right*) superimposed on axial T2*-weighted MR images of the cerebellum of a healthy subject. Lesions are flipped to the same side. Cerebellar nuclei are shown as hypointensities. * – dentate nucleus, *arrow* – interposed nucleus. Note that the interposed nucleus was preserved in the PICA group. The number of overlapping lesions is illustrated by color, from *violet* ($n = 1$) to *red* ($n = 10$ or 12)

Classical eyeblink conditioning has been shown to depend on the integrity of Larsell lobule HVI (H = hemisphere) and the interposed nucleus in animal experiments (Thompson and Steinmetz 2009 for review). Given that lobule VI and the interposed nuclei are most commonly supplied by the SCA, one would expect that SCA but not PICA patients are impaired in eyeblink conditioning. In an earlier study, it was found that this was indeed the case (Gerwig et al. 2003). Patients were tested on the lesioned and nonlesioned side. The acquisition was significantly reduced in SCA patients on their lesioned compared to their nonlesioned side (Fig. 72.4). This difference was significantly less in the PICA group. However, in the PICA group, acquisition was still lower on the lesioned compared to the nonlesioned side. The SCA commonly supplies lobules I-Crus I (with Crus I being part of lobule VIIa) and the PICA lobules Crus II-X (with Crus II also being part of lobule VIIa). There is, however, a known variability in the territories of the PICA and SCA (Amarenco 1991). Although the interposed nuclei are almost

never supplied by the PICA, Crus I can be supplied by the PICA. Crus I is also known to contribute to eyeblink conditioning. Results were "cleaner" when patients with large PICA stroke (extending into Crus I) were considered as SCA lesions. In the revised PICA group, there was no difference comparing eyeblink conditioning on the lesioned and nonlesioned side. These findings illustrate limitations of lesion-symptom maps between patients with stroke in different vascular territories. Methods independent of predefined anatomical regions are less biased.

Pooling Brain Images Based on Behavioral Cutoffs. Another way to group patients is using behavioral thresholds. That is, behavior can be defined as normal or abnormal according to comparisons with a neurological healthy control group and compare lesion sites between affected and unaffected patients. This approach was taken in a study in children and young adults with chronic surgical lesions (Konczak et al. 2005). Postural sway was assessed in different conditions. In the conditions where subjects had to rely on vestibular inputs to maintain balance, a subgroup of patients manifested excessive sway that could lead to falls or subjects stepping off the force plate. Eight of the 14 patients revealed abnormal postural sway. MRI overlays from these patients revealed that the lesioned areas involved the fastigial and interposed nuclei in 8/8 patients and dorsomedial portions of the dentate nucleus in 6/8 patients (Fig. 72.5). In the remaining six patients, whose postural sway was within the limits of the control group, the region of maximum overlap was located in paravermal regions (VIIIA, VIIIB) and only included 3/6 patients. These findings underscore the importance of fastigial nuclei (the medial zone) in postural control. However, not only the fastigial nuclei but also the interposed nuclei and, to a lesser extent, the dorsomedial part of the dentate nucleus were affected. The dorsomedial part of the dentate is thought to be part of the intermediate zone (Mason et al. 1998). Behavior results suggest that the intermediate zone may contribute to balance.

Subtraction Analysis. Subtraction analysis is a way to quantify group differences observed with brain images pooled based on behavioral cutoffs (or across predefined anatomical regions). Subtraction analysis is performed voxel-wise. For each behavioral measure and each voxel, one can say that a patient's lesion is "consistent" for that voxel if the patient is impaired and has a lesion in that voxel or if the patient is unimpaired and has no lesion in that voxel. That is, for each voxel, the patients are divided into four groups: (1) voxel lesioned, behavior normal; (2) voxel lesioned, behavior abnormal; (3) voxel extant, behavior normal; (4) voxel extant, behavior abnormal. Patients in groups (2) and (3) are consistent for this voxel while patients in groups (1) and (4) are inconsistent. The number of patients in each group is often expressed as percentages to allow comparisons independent of the size of the subject pool. Finally, the percentage of inconsistent patients is subtracted from the percentage of consistent patients. A result of 100% represents 100% consistency of patients for that voxel. That is, all patients who have a lesion that encompasses that voxel show behavioral deficit and all patients with lesions that spare that voxel have normal behavior.

Subtraction analysis has been performed both in acute cerebellar patients (Baier et al. 2009, 2010; Baier and Dieterich 2011) and in patients with chronic cerebellar lesions (Donchin et al. 2012; Werner et al. 2010). Here, one example is given which expands the above findings in posture (Konczak et al. 2005) to gait (Ilg et al. 2008).

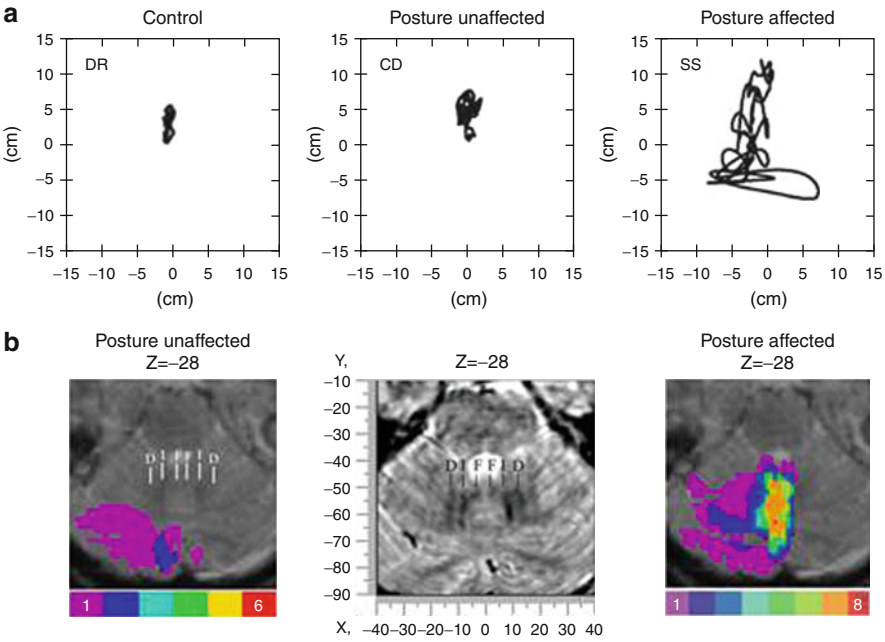

Fig. 72.5 *Pooling brain images based on behavioral cutoffs.* (**a**) Effect of nucleus fastigii lesions on postural sway (Konczak et al. 2005). In patient CD, the nuclei fastigii were intact, while lesioned in patient SS, who demonstrated excessive postural sway. Shown are the center of gravity sway paths over 20 s in one trial of a condition testing vestibular (vestibulocerebellar) function (platform sway-referenced, eyes closed). (**b**) Axial views of the region of overlap in patients with intact posture (posture unaffected) and in patients with abnormal sway area (posture affected). Note that fastigial nuclei were spared in the unaffected group. *Colors* represent the degree of overlap between patients (*red* indicating the highest overlap). Transversal section from a 3D MRI atlas of the cerebellar nuclei (Dimitrova et al. 2002) is shown for comparison. Negative z values correspond to distances in mm below the AC–PC (anterior commissure–posterior commissure) line. *D* – dentate nucleus, *I* – interposed nucleus, *F* – fastigial nuclei

All subjects had chronic surgical lesions and performed three tasks: goal-directed leg placement, walking, and walking with additional weights on the shanks. Based on the performance in the first two tasks, patients were categorized as impaired or unimpaired for leg placement and for dynamic balance control in gait. Lesion-based MRI subtraction analysis revealed that the fastigial nuclei (and to a lesser degree the interposed nuclei) were more frequently affected in patients with impaired compared to unimpaired dynamic balance control, whereas the interposed and the adjacent dentate nuclei (i.e., the intermediate zone) were more frequently affected in patients with impaired compared to unimpaired leg placement (Fig. 72.6). The subgroup with impaired leg placement but not the subgroup with impaired balance showed abnormalities in the adaptation of locomotion to additional loads. A detailed analysis revealed specific abnormalities in the temporal aspects of intralimb coordination for leg placement and adaptive locomotion.

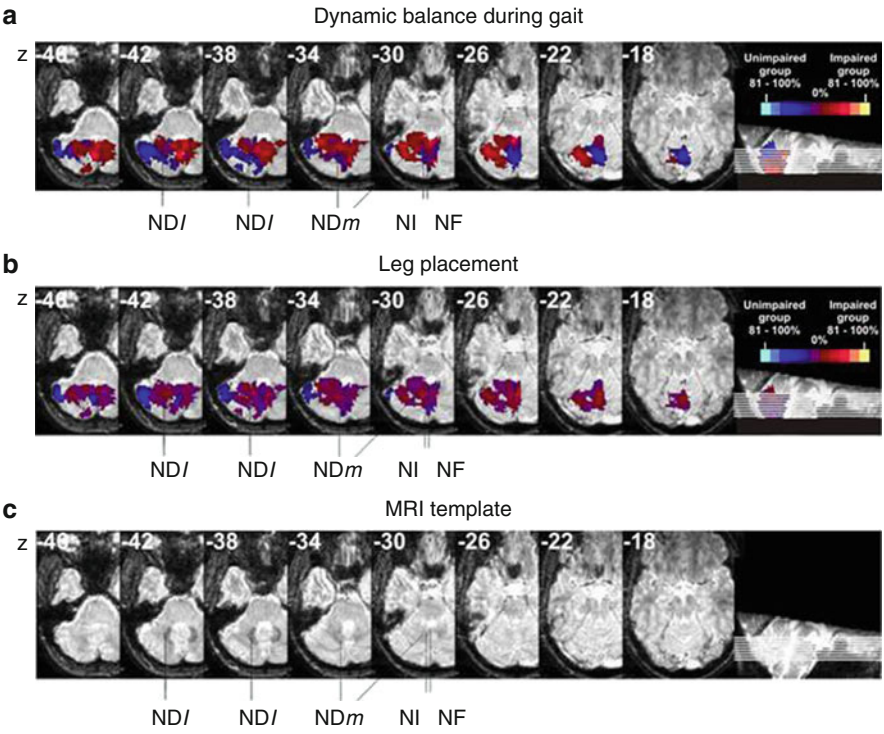

Fig. 72.6 *Subtraction analysis.* Subtraction analysis was used to reveal cerebellar areas (**a**) in dynamic balance during gait and (**b**) leg placement (Ilg et al. 2008). Brighter shades of *red*, *orange*, and *yellow* indicate regions that are commonly damaged in impaired patients but that are spared in unimpaired patients. Progressively brighter shades of *blue* illustrate the reverse situation: regions specifically damaged in unimpaired patients. *Purple* indicates regions that are damaged in equal proportions impaired and unimpaired patients. Subtraction of lesions of the six patients with impaired balance control and the six patients with unimpaired balance control showed that the lower vermis and fastigial nuclei were affected 61–80% more often in the impaired group (small area in light orange color in (**a**). A more extended area could also be defined where lesions were 41–60% more common in the affected group (*red* color). This area included the fastigial and interposed nucleus. Subtraction of lesions of the eight patients with impaired leg placement and the four patients with unimpaired leg placement showed dorsomedial parts of the dentate nucleus were affected 41–60% more often in the impaired group (*red* color in **b**). Interposed nuclei were affected 21–40% more frequently in the impaired group (middle *brown*). (**c**) Cerebellar nuclei are shown as hypointensities in the utilized MRI template (Dimitrova et al. 2002). *NF* – fastigial nucleus, *NI* – interposed nucleus, *NDl* – ventrolateral dentate nucleus, NDm – dorsomedial dentate nucleus

The intermediate zone appears thus to be of particular importance for multijoint limb control in both goal-directed leg movements and in locomotion. Furthermore, lesions of the intermediate zone may lead to disordered leg and trunk coordination, which adds to disordered balance control during stance (Konczak et al. 2005) and gait (Ilg et al. 2008).

Subtraction analysis is a useful tool in small patient populations. It has, however, two limitations. First, the method is descriptive. There is no fixed rule to decide

which level of consistency indicates a significant contribution of a region to a given behavior. Second, patients are considered either normal or abnormal. No graduation of the abnormality is done. This is useful in patients with acute disorders, because, here, behavior rapidly changes across the first days after the insult. Differences in behavior may reflect the stage of recovery but not differences in lesion localization (Rorden and Karnath 2004). However, in patients with chronic lesions, information gets lost. Some areas may be more important for a given behavior than others and are followed by more significant behavioral changes.

Voxel-wise (Inferential) Statistical Mapping

In overlay plots and subtraction analysis, no inferential statistical comparison is performed; comparisons are descriptive. Inferential statistical mapping typically requires examining a relatively large group of patients. This is due to the inherent variability in lesion volume and extent as well as difficulties in computing the true structural and functional extent of a lesion (Rorden and Karnath 2004; Rorden et al. 2007). This approach works best in chronic patients whose behavioral performance is stable (Rorden and Karnath 2004).

When the symptoms are binary (e.g., a behavior is normal or abnormal based on a behavioral cutoff), binomial tests can be performed to examine whether the spatial location of the brain lesion can predict the individual's behavioral symptoms. If symptom severity is a continuous variable, multiple *t* tests (or a nonparametric alternative) are more appropriate (Bates et al. 2003; Rorden et al. 2007). A *t* test is conducted at each voxel comparing the behavioral scores of the patients for whom that voxel is intact and lesioned on the parameter of interest. In this case, correlation between tissue damage and behavior impairment can be obtained on a voxel-by-voxel basis without needing to group patients by behavioral cutoff. Kinkingnéhun et al. (2007) have introduced a method (Anatomo-Clinical Overlapping Maps, AnaCOM), in which behavioral data of the lesioned patients is compared to control data (and is performed on a cluster of voxels rather than a voxel level for reasons given below). AnaCOM appears to be sensitive but is likely less specific than conventional methods of lesion-symptom mapping (Rorden et al. 2009).

Similar to functional MRI, voxel-wise lesion-symptom mapping has the problem of multiple comparisons. Bonferroni correction is one option to correct for multiple comparisons. Bonferroni correction is, however, very conservative, and real effects are likely to be missed. Other options are to reduce the number of comparisons and to perform more sensitive methods of corrections (Rorden et al. 2009). To reduce the number of comparisons, it is helpful to consider only those voxels which are lesioned in at least a certain number or percentage of patients ("overlap thresholding"). Cluster-of-voxels-based thresholding takes this idea even further. Here, statistical tests are calculated not on a voxel level but considering clusters of contiguous voxels that share a common overlap pattern (e.g., all contiguous voxels which are lesioned in at least three patients; Kinkingnéhun et al. 2007). Permutation thresholding is a less conservative method than Bonferroni correction and has become available in the more recent versions of NPM as part of MRIcron (http://www.sph.sc.edu/comd/rorden/mricron/; Rorden et al. 2009). Another alternative is to control for the false discovery rate (FDR)

instead of the familywise error (FWE). Rorden and coworkers favor permutation thresholding in larger group of subjects and FDR in smaller groups. More recently, voxel-based Bayesian lesion-symptom mapping has been introduced, an alternative method to conventional voxel-based lesion-symptom mapping, which does not require multiple comparison corrections (Chen and Herskovits 2010).

Binominal Data. Fisher exact test, chi-square test, and Liebermeister test are possible options to compare binominal data. In MRIcro the Yates-corrected chi-square test is implemented which closely approximates the Fisher exact test (Rorden et al. 2007). The Liebermeister test appears more sensitive than the Fisher exact test, which is more conservative. The Liebermeister test has been implemented in NPM (as part of MRIcron) by the same group.

Baier et al. (2009; Baier and Dieterich 2011) have investigated the cerebellar structures involved in oculomotor control in two larger groups of patients with acute, mainly unilateral cerebellar stroke. They used subtraction analysis to show lesion-symptom maps and applied binominal tests to prove that these findings were statistically significant. In their first study, the smooth pursuit system was investigated in 28 patients. Smooth pursuit was intact in 17 of the patients and disordered in 11. By means of Fisher exact test they found that smooth pursuit disorders were significantly related to damage of the uvula [vermal lobule (l.) IX] and vermal pyramid (vermal l. VIII) (Baier et al. 2009). In a second study, they compared the presence or absence of gaze-evoked nystagmus in 21 acute cerebellar stroke patients, with seven of them showing gaze-evoked nystagmus. The presence of gaze-evoked nystagmus was significantly related to lesions of the midline and lower cerebellar structures based on chi-square test [vermal pyramid (vermal l. VIII), uvula (vermal l. IX), and tonsil (l. IX) but also parts of the biventer lobule (l. VIII) and the inferior semilunar lobule (l. VII)]. These structures are likely part of a gaze-holding neural integrator system (Baier and Dieterich 2011).

Continuous Data. Student's *t* tests were first implemented in free software developed by Stephen Wilson called VLSM (voxel-based lesion-symptom mapping; Bates et al. 2003; http://crl.ucsd.edu/vlsm/). It is now also available in NPM developed by Chris Rorden (Rorden et al. 2007). Note, that other program packages exist to perform voxel-wise lesion-symptom mapping (e.g., BrainVox, Frank et al. 1997; VoxBo, Kimberg et al. 2007). The *t* test assumes that the data are normally distributed and is based on an interval scale. Although *t* tests are robust to violations of these assumptions (the test loses sensitivity and does not generate false positives), nonparametric tests are preferred and frequently used in these situations (e.g., Mann–Whitney U or Wilcoxon rank sum test). In NPM, the Brunner and Munzel test is offered as a nonparametric alternative to *t* tests and is supposed to be more sensitive (Rorden et al. 2007). It has been pointed out that Brunner–Munzel statistic requires at least ten subjects in both the lesion and no lesion group for each tested voxel. To correct for large type I errors (false positives), multiple comparisons need to be corrected for, and permutation-derived corrections have been recommended (Medina et al. 2010). In cerebellar lesion studies, the criterion of ten subjects in each group and any given voxel is only rarely achieved. Therefore, either Brunner–Munzel test with permutations or the more robust *t* test should be

used. Because of the multiple-comparison problem, FDR or permutation correction should be applied to the latter.

The authors applied *t* tests using voxel-based lesion-symptom software (VLSM; Bates et al. 2003) to correlate between clinical ataxia rating scores (ICARS; Trouillas et al. 1997) and MRI-defined lesions in patients with acute and chronic focal cerebellar lesions (Schoch et al. 2006). A total of 90 cerebellar patients were collected over a period of 6 years. Patients had either had a cerebellar ischemic stroke or they had undergone surgical removal of a cerebellar space-occupying process. A separate analysis was performed in patients with acute and chronic vascular ischemic lesions and patients with acute and chronic surgical lesions. The generated VLSM map displays the t scores where, by convention, large positive scores indicate that lesions in these voxels have a highly significant effect on behavior (i.e., lesioned patients perform poorly relative to intact patients). VLSM mapping of ICARS subscores revealed significant lesion-symptom correlations in acute and chronic ischemic patients and chronic surgical patients. In contrast, no significant lesion-symptom correlation was observed in the acute tumor group for reasons outlined above (section "Acute Cerebellar Lesions").

In acute ischemic patients a somatotopy in the superior cerebellar cortex was found which is in close relationship to animal data and functional MRI data in healthy control subjects (Grodd et al. 2001). Upper limb ataxia was correlated with lesions of cerebellar lobules IV–V and VI (Fig. 72.7a), lower limb ataxia with lesions of lobules III and IV, and dysarthria with lesions of lobules V and VI. As outlined above, Urban et al. (2001) created maps of lesion overlap in patients with dysarthria due to acute stroke. In good accordance to the findings above, they showed that dysarthria was related to lesions affecting the upper paravermal area of the cerebellar hemisphere.

Furthermore, in the acute lesions, limb ataxia was significantly correlated with lesions of the interposed and part of the dentate nuclei and ataxia of posture and gait with lesions of the fastigial nuclei including part of interposed nuclei. In the subgroups with chronic focal lesions, similar correlations were observed with lesions of the cerebellar nuclei, but no such correlations found for the acute group with lesions of the cerebellar cortex (Fig. 72.7b). The lesion site therefore appears to be critical for motor recovery. The remaining cerebellar symptoms in both chronic ischemic and surgical cerebellar patients are significantly correlated with lesions of the cerebellar nuclei but not the cerebellar cortex. The findings agree with clinical experience and animal studies showing that a recovery after lesions to the nuclei of the cerebellum is often less complete (Eckmiller and Westheimer 1983).

Cerebellar (Cortical) Degeneration

As yet, comparatively few human cerebellar lesion studies have used information about the local distribution of cortical cerebellar atrophy. Conventional MRI volumetry and voxel-based morphometry (VBM) are two options to assess the correlation of behavioral data and regional cerebellar atrophy. Both methods are based on T1-weighted 3D high-resolution MR images. Whereas conventional MRI

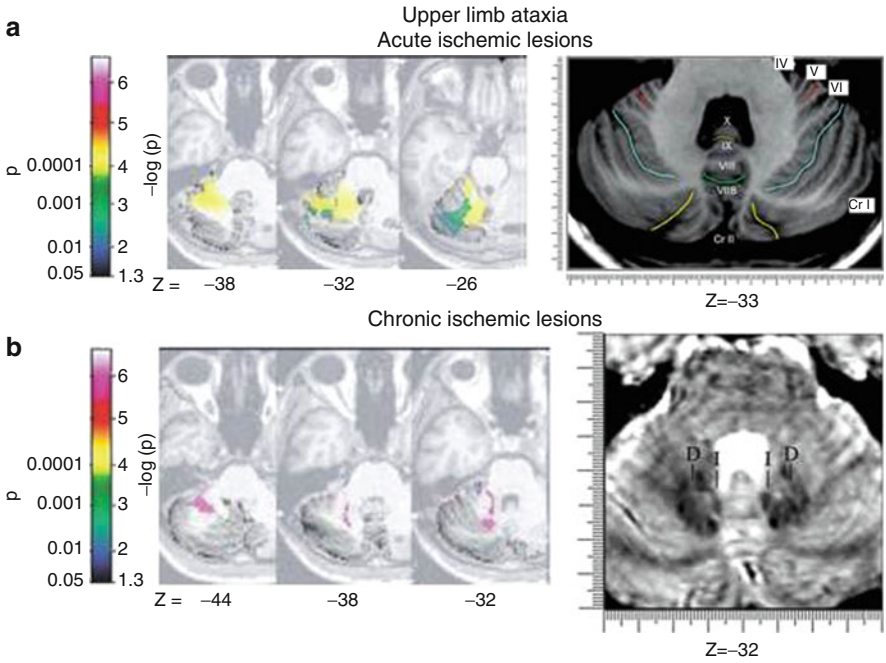

Fig. 72.7 *Voxel-based lesion-symptom mapping*. Voxel-based lesion-symptom mapping (VLSM; Bates et al. 2003) of upper limb ataxia rating score (ICARS; Trouillas et al. 1997) in (**a**) 21 subjects with acute and (**b**) 33 subjects with chronic ischemic cerebellar lesions (Schoch et al. 2006). VLSMs are superimposed on axial slices of the cerebellum of a healthy subject normalized to MNI space. Right-sided lesions are flipped to the *left*. VLSM (*p* values, Bonferroni-corrected) maps are plotted with $-\log(p) \geq 1.3$ and $p \leq 0.05$. Transversal sections from 3D MRI atlas of the cerebellum (**a**; from Schmahmann et al. 2000, Fig. 150_1_HOR-33, with permission from Elsevier) and 3D MRI atlas of the cerebellar nuclei (**b**; Dimitrova et al. 2002) are shown for comparison. *I* – interposed nucleus, *D* – dentate nucleus

volumetry accesses atrophy in predefined cerebellar regions, no anatomical regions need to be predefined in VBM. In VBM, the local concentration of gray matter is assessed on a voxel-wise basis with the potential for better spatial resolution. VBM data, however, need to be normalized to standard stereotaxic space, which is not the case in conventional volumetry. Both methods can equally be used to assess the cerebral cortex to search for accompanying extracerebellar degeneration.

Conventional Volumetric Analysis

Volumetric analysis can be performed manually, semiautomatically, and automatically using different tools in cerebellar degeneration (Luft et al. 1998; Raz et al. 2001; Brandauer et al. 2008; Schulz et al. 2010). Volumes are calculated for the whole cerebellum, cerebellar cortex, and for the white matter. The cerebellar cortex can be further subdivided (1) in the anterior and posterior cerebellum (subdivided by the primary fissure) and (2) into the medial (vermal), intermediate, and lateral

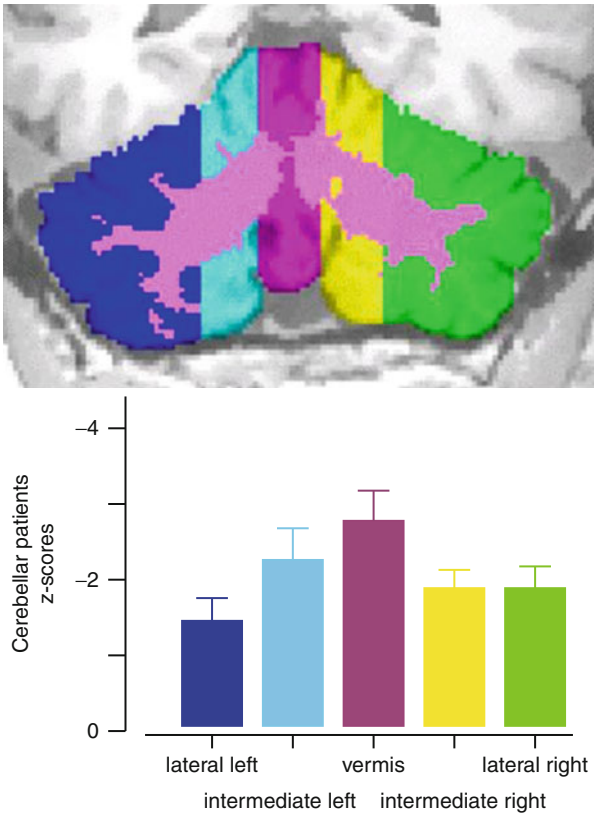

Fig. 72.8 *Conventional volumetric analysis*. *Upper row*: Subdivisions of the cerebellum: white matter (*pink*), cerebellar cortex of the lateral zone (*blue*, *green*), the intermediate zone (*light-blue*, *yellow*), and the medial zone (*purple*). *Lower row*: Degree of cerebellar atrophy in a group of 17 patients with cerebellar degeneration, expressed as (negative) Z score from a group of age- and gender-matched healthy controls (Brandauer et al. 2008). Note that the degree of atrophy was most marked in the medial cerebellum (vermis)

zones (Luft et al. 1998; see below). Volumetric analysis on the basis of individual lobule is another possibility (Makris et al. 2005). As yet, no attempts have been made to analyze the volume of the cerebellar nuclei. Volumetric data should be normalized to body size. One way is to express cerebellar volume as percentage of the total intracranial volume (Brandauer et al. 2008).

The group of the authors performs volumetric analysis of MPRAGE images of patients with cerebellar degeneration with the help of ECCET software (Brandauer et al. 2008; http://www.eccet.de). The cerebellum is semiautomatically marked and then segmented with a 3D filling algorithm. Segmentation of cerebellar cortex and white matter is performed automatically using intensity contours (Makris et al. 2005). Separation of the vermis, intermediate, and lateral cerebellum is highly standardized because there are neither anatomical landmarks to subdivide the anterior vermis and hemispheres nor the intermediate and lateral zones. After defining the midline of the cerebellum in the sagittal plane, the volume of 12 sagittal slices (six slices on the left and six on the right side of the midline) is considered vermis. The intermediate cerebellum is defined as the medial one-quarter of the maximal width of each hemisphere; the lateral cerebellum comprises the lateral three-quarters (Luft et al. 1998).

Table 72.1 Correlation of regional atrophy and two clinical ataxia scores in patients with cerebellar degeneration. Correlation coefficients (r) and corresponding *p* values are shown for sagittal cerebellar subvolumes. For the lateral and intermediate cerebellum, means of left and right cerebellar subvolumes were calculated. *ICARS* International Cooperative Ataxia Rating Scale, *SARA* Scale for the Assessment and Rating of Ataxia (From Brandauer et al. 2008, with permission)

	Subvolumes total		
Subscore	Lateral cerebellum	Intermediate cerebellum	Medial cerebellum
ICARS posture and Gait	r = −0.45	−0.65	−0.56
	$p = 0.07$	0.005	0.02
ICARS kinetic limb functions	r = −0.52	−0.51	−0.45
	$p = 0.03$	0.04	0.07
ICARS speech disorders	r = −0.65	−0.72	−0.57
	$p = 0.004$	0.001	0.02
ICARS oculomotor disorders	r = −0.28	−0.48	−0.61
	$p = 0.28$	0.05	0.01
SARA posture and gait (items 1–3)	r = −0.39	−0.59	−0.58
	$p = 0.12$	0.01	0.02
SARA speech (item 4)	r = −0.69	−0.76	−0.51
	$p = 0.002$	<0.001	0.04
SARA kinetic limb functions (items 5–8)	r = −0.67	−0.68	−0.51
	$p = 0.004$	0.003	0.04

As expected, compared to healthy subjects, patients with cerebellar degeneration have significantly smaller cerebellar volume, which is often most marked for the volume of the medial cerebellum (vermis) (Fig. 72.8; Brandauer et al. 2008). Different groups have reported significant negative correlations between total cerebellum volume or cerebellar gray matter and total clinical ataxia scores (Richter et al. 2005; Schulz et al. 2010; Lukas et al. 2011). In one study, significant correlations between ataxia subscores and functionally meaningful cerebellar subvolumes could be observed (Table 72.1; Brandauer et al. 2008). Oculomotor disorders were highly correlated with atrophy of the medial cerebellum. Posture and gait ataxia subscores revealed the highest correlations with the medial and intermediate cerebellar volume. Disorders in limb kinetic functions correlated with atrophy of lateral and intermediate parts of the cerebellum. The subscore for speech disorders showed the highest correlation with the intermediate cerebellum. All of these findings are consistent with animal data showing that the medial zone is of particular importance for control of stance, gait and eye movements, and the intermediate and lateral zones for control of limb movements and speech (Thach et al. 1992). Atrophy of the intermediate zone, however, was correlated not only with limb ataxia and dysarthria but also with ataxia of stance and gait. This agrees with the studies in subjects with chronic focal cerebellar lesions cited above. These studies revealed that postural sway and disordered balance control during gait were

associated with lesions affecting both the fastigial (medial zone) and interposed nuclei (intermediate zone) (Konczak et al. 2005; Ilg et al. 2008).

Voxel-Based Morphometry (VBM)

VBM has become a major tool to demonstrate gray matter changes in disorders with no obvious abnormalities in structural MRI (Rorden and Karnath 2004). It is analyzed whether different experimental groups (here, patients versus controls) have different tissue concentrations. Because atrophy of the cerebellum is obvious in structural MRI, this is less an issue in behavioral studies in cerebellar degeneration. More interestingly, correlation analysis between morphometric data and behavioral scores can be performed. As yet, VBM has rarely been used in cerebellar lesion studies. It has been questioned whether standard normalization algorithms, a necessary prerequisite for VBM analysis, will work in patients suffering from severe morphological pathology such as cerebellar atrophy. This appears to be the case. First, VBM has been used in patients with spinocerebellar ataxia type 6 and has shown the expected gray matter loss in the cerebellar cortex (Lukas et al. 2006; Schulz et al. 2010). Second, a meaningful significant negative correlation between clinical ataxia scores and cerebellar structures has been found in spinocerebellar ataxia type 17 (Lasek et al. 2006).

Recently, the SUIT toolbox in SPM has become available for normalization of VBM data (http://www.icn.ucl.ac.uk/motorcontrol/imaging/suit_vbm.htm). As outlined above, SUIT offers improved normalization of the cerebellar cortex. For each patient, the quantity of gray matter is calculated that maps from that patient's MRI scan onto each voxel in the SUIT atlas. It will be of interest to apply SUIT-VBM to determine patterns of cerebellar degeneration and their correlation to behavioral disorders in future studies. Note that VBM is also of interest in patients with chronic focal cerebellar disorders. VBM is a useful option to access secondary changes in preserved cerebellar tissue and in connected cerebral areas (Clausi et al. 2009).

Structural Connectivity of Cerebellar Pathways

Lesion-symptom mapping as outlined above focuses on assessment of structural changes of the cerebellar gray matter (cortex and nuclei) and possible correlations to behavioral disorders. MR diffusion tensor imaging (DTI) enables the study of connecting white matter tracts of the cerebellum and possible abnormalities in vivo. Connections of the dentate nucleus via thalamus to the prefrontal neocortex, found in histological studies in monkey (Dum and Strick 2003), have been confirmed in healthy human subjects using DTI (Habas and Cabanis 2007; Jissendi et al. 2008). In addition, connections of the dentate nucleus to the red nucleus and mammillary tubercle have been visualized (Habas and Cabanis 2007). Granziera et al. (2009) have used diffusion spectrum imaging (DSI), which has advantages compared to the wider used DTI in imaging of crossing fibers, in order to identify functional cerebellar circuits. In this study, afferent connections from the inferior olive to the dentate nucleus and from the cerebellar cortex to all cerebellar nuclei according to

the known parasagittal zones have been visualized. In addition, efferent pathways from the cerebellar nuclei to the ventrolateral thalamus and red nucleus and their output through the three cerebellar peduncles were shown.

Changes of structural connectivity have been found in patients with chronic focal cerebellar lesions (Rueckriegel et al. 2010) and in patients with various forms of cerebellar degeneration (most of them not confined to the cerebellum; Kitamura et al. 2008; Alcauter et al. 2011). Very few behavioral studies have tried to correlate behavioral findings and DTI data of cerebellar pathways. Della-Maggiore et al. (2009) found in healthy subjects that fractional anisotropy (FA) correlated with the rate of adaptation to an optical rotation in a region consistent with the superior cerebellar peduncle. As yet, no human cerebellar lesion studies attempted to quantify changes in connectivity and assess possible relations to behavioral data. In patients both with focal and degenerative cerebellar lesions, it will be of interest to include structural connectivity MRI in future studies.

Atlases of the Cerebellar Cortex and Nuclei

Atlases are used to allocate regions found in lesion-symptom maps to anatomical areas within the cerebellum. Because analysis is based on spatially normalized lesions, atlases are needed which show the cerebellum in the same stereotactic space. The first 3D MRI atlas of the human cerebellum in proportional stereotaxic MNI space was introduced by Schmahmann et al. (2000). This atlas was a helpful complement to the widely used atlas of Talairach and Tournoux (1988) where no anatomic structures are specified within the sketched outlines of the cerebellum. For many years, Schmahmann et al.'s atlas was a major tool in identifying cerebellar lobules and fissures in functional and structural imaging studies (e.g., see Fig. 72.7). However, some limitations applied. Firstly, it was based on one single subject and did not take individual variations of the cerebellar cortex into account. Secondly, the atlas is not spatially unbiased, that is, atlas and MNI coordinates cannot be treated the same (http://www.icn.ucl.ac.uk/motorcontrol/imaging/suit.htm). These shortcomings have been addressed by Diedrichsen et al. (2009) who have published the first probabilistic atlas of the cerebellar cortex (http://www.icn.ucl.ac.uk/motorcontrol/imaging/propatlas.htm; Fig. 72.9). The atlas is based on the cerebella of 20 healthy subjects in which individual lobules are outlined. The atlas is available in different versions for imaging data normalized to the SUIT or MNI template. It differentiates between vermis and hemispheres.

In the 3D MRI atlas of the human cerebellum introduced by Schmahmann et al. (2000), the cerebellar nuclei are not visible on the MRI scans. Digitized autopsy cryosections of other cerebella turned into Talairach space are used instead. Dimitrova et al. (2002) introduced a 3D MRI-based atlas of the cerebellar nuclei in MNI space. The atlas is based on a single female subject (age 26 years) imaged with a T2*-weighted fast low-angle shot sequence (FLASH) acquired five times and averaged to improve signal to noise ratio (see Figs. 72.4 and 72.6). To take individual variations in localization, size, and shape of the cerebellar nuclei into

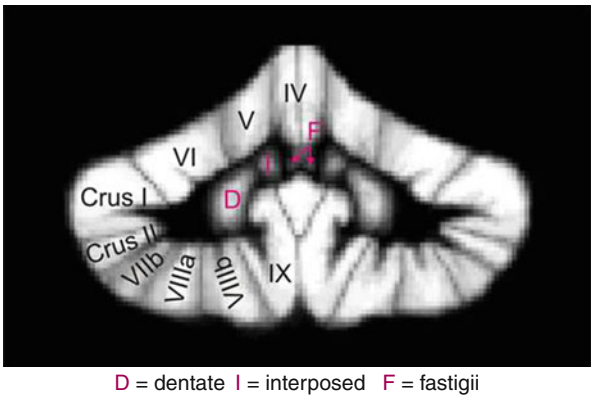

Fig. 72.9 Coronal slice of the combined probabilistic atlas of the cerebellar cortex (Diedrichsen et al. 2009) and the cerebellar nuclei (Diedrichsen et al. 2011) which is freely available (http://www.icn.ucl.ac.uk/motorcontrol/imaging/propatlas.htm; with permission from J. Diedrichsen). The maximum probability maps are shown in SUIT space and for the image viewer MRICron (http://www.cabiatl.com/mricro/mricron/). The atlas is also available for MNI space and for the programs SPM and FSL

account the same group developed a probabilistic atlas of the dentate and interposed nuclei based on 63 healthy subjects (Dimitrova et al. 2006). Standard statistical parametric mapping (SPM, www.fil.ion.ucl.ac.uk/spm/) normalization techniques were used, and the probabilistic atlas was created by simple overlap of individual nuclei. Dentate and interposed nuclei were not separated, and the fastigial nuclei were not included. These shortcomings are addressed in the most recent probabilistic atlas of the cerebellar nuclei (Diedrichsen et al. 2011; http://www.icn.ucl.ac.uk/motorcontrol/imaging/propatlas.htm; Fig. 72.9). The anatomical data collection was based on ultrahigh-field (7 T) MR high-resolution SWI images in the submillimeter range (0.5 mm isotropic). The dentate nucleus was separated from the interposed and fastigial nuclei, and the latter are included in the probabilistic atlas. Individual nuclei were normalized using different normalization methods including SPM and SUIT (see section "Normalization of the Cerebellar Cortex and Nuclei"). That is, similar to the atlas of the cortex, the atlas of the nuclei is available in MNI and SUIT space. Different measures were used to compare the quality of overlap and create the probabilistic atlas.

Conclusions and Future Directions

A traditional approach to elucidate the function of the human brain, and the cerebellum in particular, is to study impairment in human subjects with brain lesions. The approach suffers from a number of well-known limitations (Shallice 1988). The cerebellum is part of a more extended brain circuitry. Thus, a specific

behavioral deficit following a localized cerebellar lesion may result from functional disruption anywhere within that circuitry. Furthermore, in patients with chronic lesions, plasticity within the cerebellum and the connected areas may lead to changes in their function as the brain attempts to recover. In patients with acute focal lesions, changes due to neural plasticity are not a problem. However, a temporary dysfunction in connected brain areas after abrupt changes in input is a serious problem in this patient group.

Although function of the cerebellum cannot be inferred from lesion data alone, it is still of major scientific and clinical interest if lesions of a given cerebellar area lead to specific behavioral deficits. The introduction of high-resolution structural brain imaging and new analysis methods has lead to significant improvement in the ability to draw such conclusions (Rorden and Karnath 2004). Although studies of patients with focal cerebellar lesions allow for a better lesion localization, examining patients with degenerative disorders can also lead to meaningful results. Focal lesions studies can also lead to additional information about the function of the cerebellar cortex and nuclei. Application of new MRI techniques will improve definition of lesion extent even further. For example, signal-to-noise ratio increases with increasing field strength and allows spatial resolution in the submillimeter range. Additionally, susceptibility artifacts increase and allow better visualization of the cerebellar nuclei. The technique of fiber tract mapping from DTI MRI has only recently been taken up in patients with cerebellar disorders. At the same time, current developments of data analysis tools improve precision of lesion-symptom maps. In particular, normalization methods have been introduced which are specifically developed for normalization of cerebellar cortex and nuclei (Diedrichsen 2006; Diedrichsen et al. 2011). Probabilistic atlases using the same optimized normalization methods have been developed (Diedrichsen et al. 2009, 2011). Finally, statistical analysis tools are steadily improving for other applications and can be equally applied for cerebellar lesion studies (Rorden and Karnath 2004; Rorden et al. 2009). As a result of these improvements, human cerebellar lesion studies have regained much interest. Use of these advanced techniques of lesion-symptom mapping has already led to significant improvement of the current understanding of motor and cognitive function of the human cerebellum (Donchin et al. 2012; Baier et al. 2010; Küper et al. 2011b) and will help future studies to gain further inside into the pathophysiology of the cerebellum.

References

Abele M, Minnerop M, Urbach H et al (2007) Sporadic adult onset ataxia of unknown etiology: a clinical, electrophysiological and imaging study. J Neurol 254:1384–1389

Alcauter S, Barrios FA, Díaz R et al (2011) Gray and white matter alterations in spinocerebellar ataxia type 7: an in vivo DTI and VBM study. Neuroimage 55:1–7

Amarenco P (1991) The spectrum of cerebellar infarctions. Neurology 41:973–979

Amarenco P, Rosengart A, DeWitt LD et al (1993) Anterior inferior cerebellar artery territory infarcts. Mechanisms and clinical features. Arch Neurol 50:154–161

Anderson SW, Damasio H, Tranel D (1990) Neuropsychological impairments associated with lesions caused by tumor or stroke. Arch Neurol 47:397–405
Baier B, Dieterich M (2011) Incidence and anatomy of gaze-evoked nystagmus in patients with cerebellar lesions. Neurology 76:361–365
Baier B, Stoeter P, Dieterich M (2009) Anatomical correlates of ocular motor deficits in cerebellar lesions. Brain 132:2114–2124
Baier B, Dieterich M, Stoeter P et al (2010) Anatomical correlate of impaired covert visual attentional processes in patients with cerebellar lesions. J Neurosci 30:3770–3776
Barkhof F, Scheltens P (2002) Imaging of white matter lesions. Cerebrovasc Dis 2:21–30
Barth A, Bogousslavsky J, Regli F (1993) The clinical and topographic spectrum of cerebellar infarcts: a clinical-magnetic resonance imaging correlation study. Ann Neurol 33: 451–456
Bates E, Wilson SM, Saygin AP et al (2003) Voxel-based lesion-symptom mapping. Nat Neurosci 6:448–450
Brain Development Cooperative Group (2011) Total and regional brain volumes in a population-based normative sample from 4 to 18 years: the NIH MRI study of normal brain development. Cereb Cortex 22:1–12
Brandauer B, Hermsdörfer J, Beck A et al (2008) Impairments of prehension kinematics and grasping forces in patients with cerebellar degeneration and the relationship to cerebellar atrophy. Clin Neurophysiol 119:2528–2537
Brett M, Leff AP, Rorden C et al (2001) Spatial normalization of brain images with focal lesions using cost function masking. Neuroimage 14:486–500
Caplan LR (1996) Cerebellar infarcts. In: Caplan LR (ed) Posterior circulation disease: clinical findings, diagnosis, and management. Blackwell Scientific, Cambridge, MA, pp 492–543
Chaves CJ, Caplan LR, Chung CS et al (1994) Cerebellar infarcts in the New England Medical Center Posterior Circulation Stroke Registry. Neurology 44:1385–1390
Chen R, Herskovits EH (2010) Voxel-based Bayesian lesion-symptom mapping. Neuroimage 49:597–602
Clausi S, Bozzali M, Leggio MG et al (2009) Quantification of gray matter changes in the cerebral cortex after isolated cerebellar damage: a voxel-based morphometry study. Neuroscience 162:827–835
Conway JE, Chou D, Clatterbuck RE et al (2001) Hemangioblastomas of the central nervous system in von Hippel–Lindau syndrome and sporadic disease. Neurosurgery 48:55–62
Della-Maggiore V, Scholz J, Johansen-Berg H et al (2009) The rate of visuomotor adaptation correlates with cerebellar white-matter microstructure. Hum Brain Mapp 30:4048–4053
Deoni SC, Catani M (2007) Visualization of the deep cerebellar nuclei using quantitative T1 and rho magnetic resonance imaging at 3 Tesla. Neuroimage 37:1260–1266
Diedrichsen J (2006) A spatially unbiased atlas template of the human cerebellum. Neuroimage 33:127–138
Diedrichsen J, Balsters JH, Flavell J et al (2009) A probabilistic MR atlas of the human cerebellum. Neuroimage 46:39–46
Diedrichsen J, Maderwald S, Küper M et al (2011) Imaging the deep cerebellar nuclei: a probabilistic atlas and normalization procedure. Neuroimage 54:1786–1794
Dimitrova A, Weber J, Redies C et al (2002) MRI atlas of the human cerebellar nuclei. Neuroimage 17:240–255
Dimitrova A, Zeljko D, Schwarze F et al (2006) Probabilistic 3D MRI atlas of the human cerebellar dentate/interposed nuclei. Neuroimage 30:12–25
Donchin O, Rabe K, Diedrichsen J et al (2012) Cerebellar regions involved in adaptation to force field and visuomotor perturbation. J Neurophysiol 107:134–147
Dum RP, Strick PL (2003) An unfolded map of the cerebellar dentate nucleus and its projections to the cerebral cortex. J Neurophysiol 89:634–639
Durr A (2010) Autosomal dominant cerebellar ataxias: polyglutamine expansions and beyond. Lancet Neurol 9:885–894

Eckmiller R, Westheimer G (1983) Compensation of oculomotor deficits in monkeys with neonatal cerebellar ablations. Exp Brain Res 49:315–326
Exner C, Weniger G, Irle E (2004) Cerebellar lesions in the PICA but not SCA territory impair cognition. Neurology 63:2132–2135
Fiez JA, Damasio H, Grabowski TJ (2000) Lesion segmentation and manual warping to a reference brain: intra- and interobserver reliability. Hum Brain Mapp 9:192–211
Frank RJ, Damasio H, Grabowski TJ (1997) Brainvox: an interactive, multimodal visualization and analysis system for neuroanatomical imaging. Neuroimage 5:13–30
Gerwig M, Dimitrova A, Kolb FP et al (2003) Comparison of eyeblink conditioning in patients with superior and posterior inferior cerebellar lesions. Brain 126:71–94
Giedd JN, Snell JW, Lange N et al (1996) Quantitative magnetic resonance imaging of human brain development: ages 4–18. Cereb Cortex 6:551–560
Granziera C, Schmahmann JD, Hadjikhani N et al (2009) Diffusion spectrum imaging shows the structural basis of functional cerebellar circuits in the human cerebellum in vivo. PLoS One 4:e5101
Grodd W, Hülsmann E, Lotze M et al (2001) Sensorimotor mapping of the human cerebellum: fMRI evidence of somatotopic organization. Hum Brain Mapp 13:55–57
Habas C, Cabanis EA (2007) Cortical projection to the human red nucleus: complementary results with probabilistic tractography at 3 T. Neuroradiol 49:777–784
Ilg M, Giese MA, Gizewski ER et al (2008) The influence of focal cerebellar lesions on the control and adaptation of gait. Brain 131:2913–2927
Jernigan TL, Tallal P (1990) Late childhood changes in brain morphology observable with MRI. Dev Med Child Neurol 32:379–385
Jissendi P, Baudry S, Balériaux D (2008) Diffusion tensor imaging (DTI) and tractography of the cerebellar projections to prefrontal and posterior parietal cortices: a study at 3 T. J Neuroradiol 35:42–50
Karnath HO, Steinbach JP (2011) Do brain tumors allow valid conclusions on the localization of human brain functions? – objections. Cortex 47:1004–1006
Karnath HO, Himmelbach M, Rorden C (2002) The subcortical anatomy of human spatial neglect: putamen, caudate nucleus and pulvinar. Brain 125:350–360
Karnath HO, Zopf R, Johannsen L et al (2005) Normalized perfusion MRI to identify common areas of dysfunction: patients with basal ganglia neglect. Brain 128:2462–2469
Kase CS, Norrving B, Levine SR et al (1993) Cerebellar infarction. Clinical and anatomic observations in 66 cases. Stroke 24:76–83
Kimberg DY, Coslett HB, Schwartz MF (2007) Power in voxel-based lesion-symptom mapping. J Cogn Neurosci 19:1067–1080
Kinkingnéhun S, Volle E, Pélégrini-Issac M et al (2007) A novel approach to clinical-radiological correlations: Anatomo-Clinical Overlapping Maps (AnaCOM): method and validation. Neuroimage 37:1237–1249
Kitamura K, Nakayama K, Kosaka S et al (2008) Diffusion tensor imaging of the cortico-ponto-cerebellar pathway in patients with adult-onset ataxic neurodegenerative disease. Neuroradiology 50:285–292
Klockgether T (2008) The clinical diagnosis of autosomal dominant spinocerebellar ataxias. Cerebellum 7:101–105
Konczak J, Schoch B, Dimitrova A et al (2005) Functional recovery of children and adolescents after cerebellar tumor resection. Brain 128:1428–1441
Küper M, Thürling M, Maderwald S et al (2010) Structural and functional magnetic resonance imaging of the human cerebellar nuclei. Cerebellum (Epub ahead of print)
Küper M, Dimitrova A, Thürling M et al (2011a) Evidence for a motor and a non-motor domain in the human dentate nucleus–an fMRI study. Neuroimage 54:2612–2622
Küper M, Brandauer B, Thürling M et al (2011b) Impaired prehension is associated with lesions of the superior and inferior hand representation within the human cerebellum. J Neurophysiol 105:2018–2029

Lasek K, Lencer R, Gaser C et al (2006) Morphological basis for the spectrum of clinical deficits in spinocerebellar ataxia 17 (SCA17). Brain 129:2341–2352
Lechtenberg R, Gilman S (1978) Speech disorders in cerebellar disease. Ann Neurol 3:285–290
Leggio MG, Tedesco AM, Chiricozzi FR et al (2008) Cognitive sequencing impairment in patients with focal or atrophic cerebellar damage. Brain 131:1332–1343
Luft AR, Skalej M, Welte D et al (1998) A new semiautomated, three-dimensional technique allowing precise quantification of total and regional cerebellar volume using MRI. Magn Reson Med 40:143–151
Lukas C, Schöls L, Bellenberg B et al (2006) Dissociation of grey and white matter reduction in spinocerebellar ataxia type 3 and 6: a voxel-based morphometry study. Neurosci Lett 408: 230–235
Lukas C, Bellenberg B, Köster O et al (2011) A new sulcus-corrected approach for assessing cerebellar volume in spinocerebellar ataxia. Psychiatry Res 193:123–130
Makris N, Schlerf JE, Hodge SM et al (2005) MRI-based surface-assisted parcellation of human cerebellar cortex: an anatomically specified method with estimate of reliability. Neuroimage 25:1146–1160
Marinkovic S, Kovacevic M, Gibo H et al (1995) The anatomical basis for the cerebellar infarcts. Surg Neurol 44:450–460
Mason R, Miller LE, Baker JF et al (1998) Organization of reaching and grasping movements in the primate cerebellar nuclei as revealed by focal muscimol inactivations. J Neurophysiol 79:537–544
Medina J, Kimberg DY, Chatterjee A et al (2010) Inappropriate usage of the Brunner-Munzel test in recent voxel-based lesion-symptom mapping studies. Neuropsychologia 48:341–343
Pfefferbaum A, Mathalon DH, Sullivan EV et al (1994) A quantitative magnetic resonance imaging study of changes in brain morphology from infancy to late adulthood. Arch Neurol 51:874–887
Rashidi M, DaSilva VR, Minagar A et al (2003) Nonmalignant pediatric brain tumors. Curr Neurol Neurosci Rep 3:200–205
Ravizza SM, McCormick CA, Schlerf JE et al (2006) Cerebellar damage produces selective deficits in verbal working memory. Brain 129:306–320
Raz N, Gunning-Dixon F, Head D et al (2001) Age and sex differences in the cerebellum and the ventral pons: a prospective MR study of healthy adults. AJNR Am J Neuroradiol 22: 1161–1167
Richter S, Dimitrova A, Maschke M et al (2005) Degree of cerebellar ataxia correlates with three-dimensional mri-based cerebellar volume in pure cerebellar degeneration. Eur Neurol 54:23–27
Riva D, Giorgi C (2000) The cerebellum contributes to higher functions during the development: evidence from a series of children surgically treated for posterior fossa tumors. Brain 123: 1051–1061
Rorden C, Karnath HO (2004) Using human brain lesions to infer function: a relic from a past era in the fMRI age? Nat Rev Neurosci 5:813–819
Rorden C, Karnath HO, Bonilha L (2007) Improving lesion-symptom mapping. J Cogn Neurosci 19:1081–1088
Rorden C, Fridriksson J, Karnath HO (2009) An evaluation of traditional and novel tools for lesion behavior mapping. Neuroimage 44:1355–1362
Rüb U, Brunt ER, Petrasch-Parwez E et al (2006) Degeneration of ingestion-related brainstem nuclei in spinocerebellar ataxia type 2, 3, 6 and 7. Neuropathol Appl Neurobiol 32:635–649
Rueckriegel SM, Driever PH, Blankenburg F et al (2010) Differences in supratentorial damage of white matter in pediatric survivors of posterior fossa tumors with and without adjuvant treatment as detected by magnetic resonance diffusion tensor imaging. Int J Radiat Oncol Biol Phys 76:859–866
Sasaki H, Kojima H, Yabe I et al (1998) Neuropathological and molecular studies of spinocerebellar ataxia type 6 (SCA6). Acta Neuropathol (Berl) 95:199–204
Schmahmann JD, Doyon J, Toga AW et al (2000) MRI atlas of the human cerebellum. Academic Press, San Diego

Schoch B, Dimitrova A, Gizewski ER et al (2006) Functional localization in the human cerebellum based on voxelwise statistical analysis: a study of 90 patients. Neuroimage 30:36–51
Schöls L, Linnemann C, Globas C (2008) Electrophysiology in spinocerebellar ataxias: spread of disease and characteristic findings. Cerebellum 7:198–203
Schulz JB, Borkert J, Wolf S et al (2010) Visualization, quantification and correlation of brain atrophy with clinical symptoms in spinocerebellar ataxia types 1, 3 and 6. Neuroimage 49:158–168
Seghier ML, Ramlackhansingh A, Crinion J et al (2008) Lesion identification using unified segmentation-normalization models and fuzzy clustering. Neuroimage 41:1253–1266
Shallice T (1988) From neuropsychology to mental structure. Cambridge University Press, Cambridge/New York/Melbourne
Steinlin M, Imfeld S, Zulauf P et al (2003) Neuropsychological long-term sequelae after posterior fossa tumor resection during childhood. Brain 126:1998–2008
Talairach J, Tournoux P (1988) Co-planar stereotaxic atlas of the human brain. Georg Thieme, New York
Tatu L, Moulin T, Bogousslavsky J et al (1996) Arterial territories of human brain: brainstem and cerebellum. Neurology 47:1125–1135
Thach WT, Kane SA, Mink JW et al (1992) Cerebellar output, multiple maps and modes of control in movement coordination. In: Llinas R, Sotelo C (eds) The cerebellum revisited. Springer, New York/Heidelberg, pp 283–300
Thompson RF, Steinmetz JE (2009) The role of the cerebellum in classical conditioning of discrete behavioral responses. Neuroscience 162:732–755
Thürling M, Küper M, Stefanescu R et al (2011) Activation of the dentate nucleus in a verb generation task: a 7 T MRI study. Neuroimage 57:1184–1191
Timmann D, Konczak J, Ilg W et al (2009) Current advances in lesion-symptom mapping of the human cerebellum. Neuroscience 162:836–851
Tohgi H, Takahashi S, Chiba K et al (1993) Cerebellar infarction. Clinical and neuroimaging analysis in 293 patients. The Tohoku Cerebellar Infarction Study Group. Stroke 24:1697–1670
Trouillas P, Takayanagi T, Hallett M et al (1997) International Cooperative Ataxia Rating Scale for pharmacological assessment of the cerebellar syndrome. The Ataxia Neuropharmacology Committee of the World Federation of Neurology. J Neurol Sci 145:205–211
Urban PP, Wicht S, Vukurevic G et al (2001) Dysarthria in acute ischemic stroke: lesion topography, clinicoradiologic correlation, and etiology. Neurology 56:1021–1027
Vogt O (1905) Die myelogenetische Gliederung des Cortex cerebelli. J Psychol Neurol Bd V, Heft 6:235–250
Werner S, Bock O, Gizewski ER et al (2010) Visuomotor adaptive improvement and aftereffects are impaired differentially following cerebellar lesions in SCA and PICA territory. Exp Brain Res 201:429–439
Wilke M, de Haan B, Juenger H et al (2011) Manual, semi-automated, and automated delineation of chronic brain lesions: a comparison of methods. Neuroimage 56:2038–2046
Wintermark M, Albers GW, Alexandrov AV et al (2008) Acute stroke imaging research roadmap. Stroke 39:1621–1628
Yang Q, Hashizume Y, Yoshida M et al (2000) Morphological Purkinje cell changes in spinocerebellar ataxia type 6. Acta Neuropathol (Berl) 100:371–376
Zuzak TJ, Poretti A, Drexel B et al (2008) Outcome of children with low-grade cerebellar astrocytoma: long-term complications and quality of life. Childs Nerv Syst 24:1447–1455